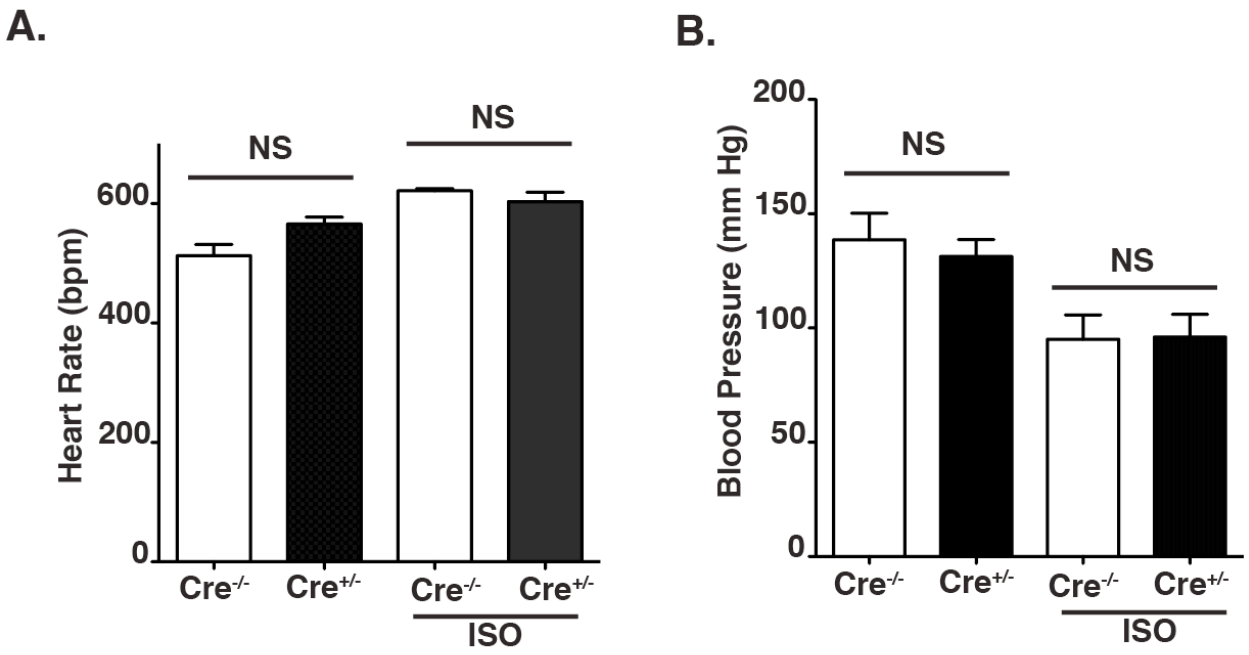

Figure S1. Depletion of PHD2 and 3 has no effect on the heart rate and blood pressure. PHD2/3$^{f/f}$; Cre$^{-/-}$ or PHD2/3$^{f/f}$; Cre$^{+/-}$ mice were IP injected with tamoxifen for 5 consecutive days. At day 7, heart rates **(A)** and systolic blood pressures (SBP) **(B)** were obtained at baseline and 5 minutes after isoproterenol treatment (3mg/kg). n = 4, NS, not significant, two way ANOVA.

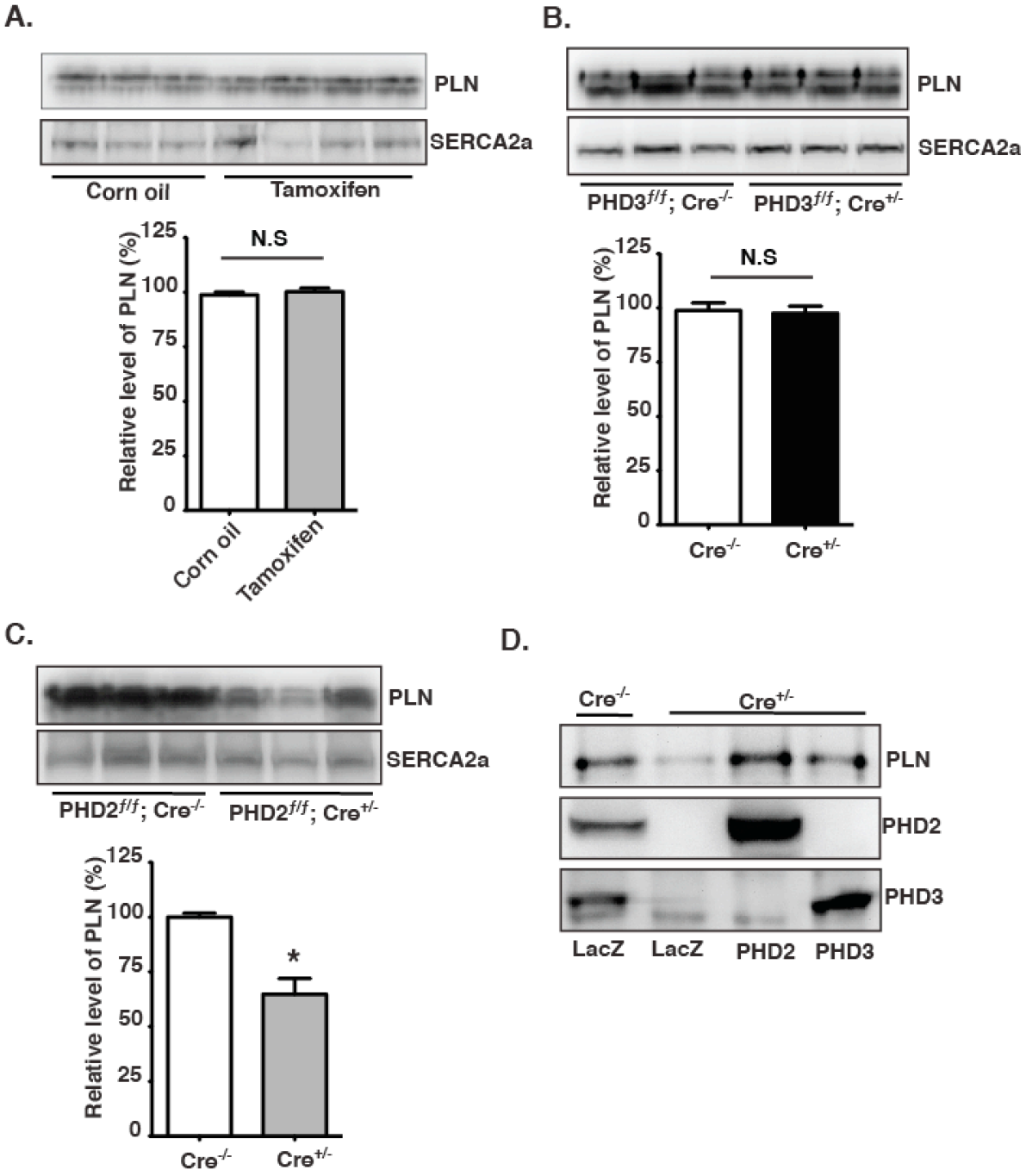

Figure S2. Differential role of PHD2 and PHD3 in regulating PLN protein level. PHD2/3$^{f/f}$; Cre$^{-/-}$ **(A)**, PHD3$^{f/f}$; Cre$^{+/-}$ **(B)** and PHD2$^{f/f}$; Cre$^{+/-}$ **(C)** mice were IP injected with tamoxifen for 5 consecutive days. At day 7, mouse hearts were harvested and western blots were performed. Densitometry analysis of the protein level of PLN was shown in the bar graph. n = 3, $^{*}p < 0.01$; N.S, not significant, 2-tailed Student's *t* test. **(D)** Neonatal ventricular myocytes isolated from PHD2/3$^{f/f}$; Cre$^{-/-}$ or PHD2/3$^{f/f}$; Cre$^{+/-}$ mice were infected with adenovirus expressing LacZ, PHD2 or PHD3 before treatment with 4-OHT for 5 days. Cells were then harvested and western-blots were performed.

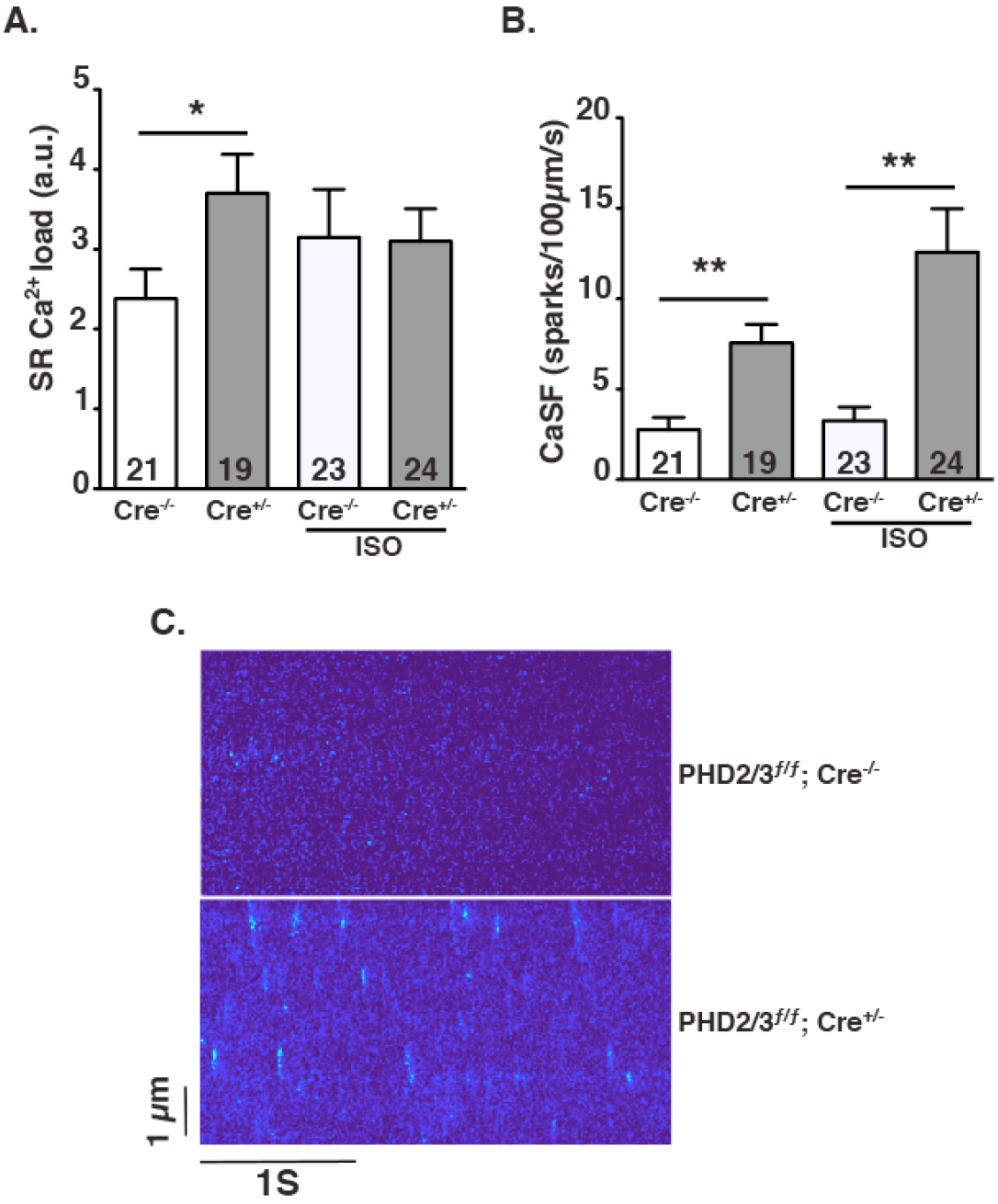

Figure S3. Depletion of PHD2 and 3 increases SR Ca^{2+} load and enhances RyR2 Ca^{2+}-release activity. PHD2/3$^{f/f}$; Cre$^{-/-}$ or PHD2/3$^{f/f}$; Cre$^{+/-}$ mice were IP injected with tamoxifen for 5 consecutive days. At day 7, mouse hearts were removed and cardiomyocytes were isolated for measuring the SR Ca^{2+} content **(A)** and Ca^{2+}-spark frequency **(B)**. Numbers inside bars indicate number of cells studied from 4 mice per group. $^{*}P<0.05$, $^{**}P<0.01$, two way ANOVA. **(C)** Representative line-scan images of Ca^{2+} -spark recordings in isolated adult ventricular cardiomyocytes at basal condition.

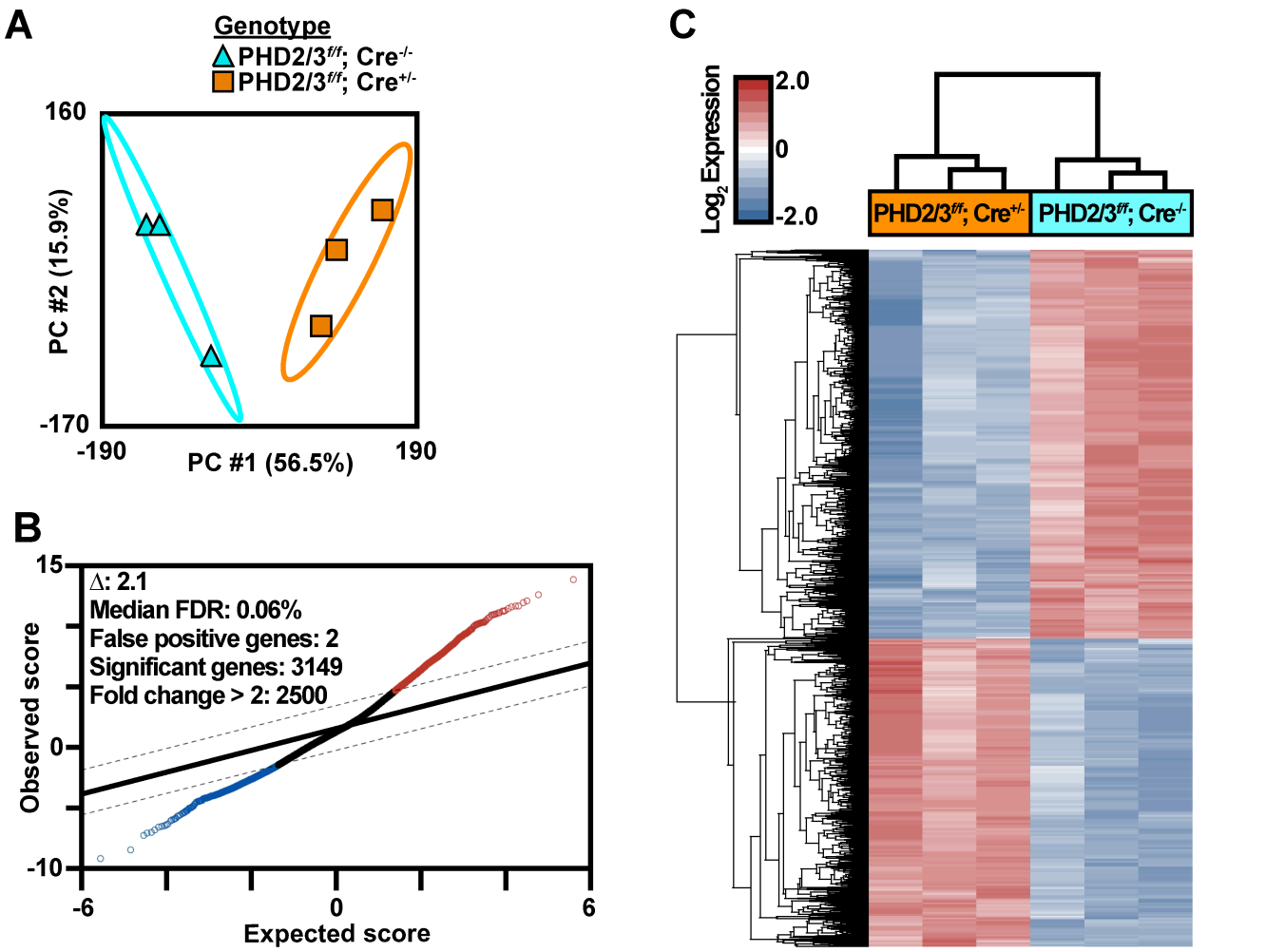

Figure S4. Whole heart gene expression microarray analysis of PHD2/3; Cre$^{+/-}$ mice. (A) Principal component analysis (PCA) of global changes in cardiac gene expression was performed on the gene expression profiles of eight week-old PHD2/3$^{f/f}$; Cre$^{-/-}$ or PHD2/3$^{f/f}$; Cre$^{+/-}$ mouse hearts (n=3 per genotype) and represented by a scatter plot of the first (PC #1) versus second principal component (PC #2). The confidence ellipses represent two standard deviations. **(B)** SAM plot of observed scores plotted against the expected scores. The solid line represents observed=expected expression values, whereas the hashed lines indicate the significance threshold based on Δ=2.1. The genes identified as differentially expressed are indicated by red and blue open circles, indicating higher and lower expression, respectively, of these genes in PHD2/3$^{f/f}$; Cre$^{+/-}$ mouse hearts. The number of differentially expressed genes, predicted false positives, and the false discovery rate (FDR) are provided. **(C)** The expression values from the 2500 genes (rows) from the six heart samples (columns) detected as differentially expressed via SAM analysis with an absolute fold change > 2 were analyzed with hierarchical clustering using the Euclidian matrix with average linkage (Partek Genomics Suite, v6.6). As expected based on the 2 class unpaired SAM analysis used to identify differentially expressed genes, we identified 2 primary clusters of microarray samples comprised solely of either PHD2/3$^{f/f}$; Cre$^{-/-}$ or PHD2/3$^{f/f}$; Cre$^{+/-}$ biological replicates. Additionally, the genes portioned into 2 groups of higher (maroon) or lower (blue) expression across the 2 genotypes.

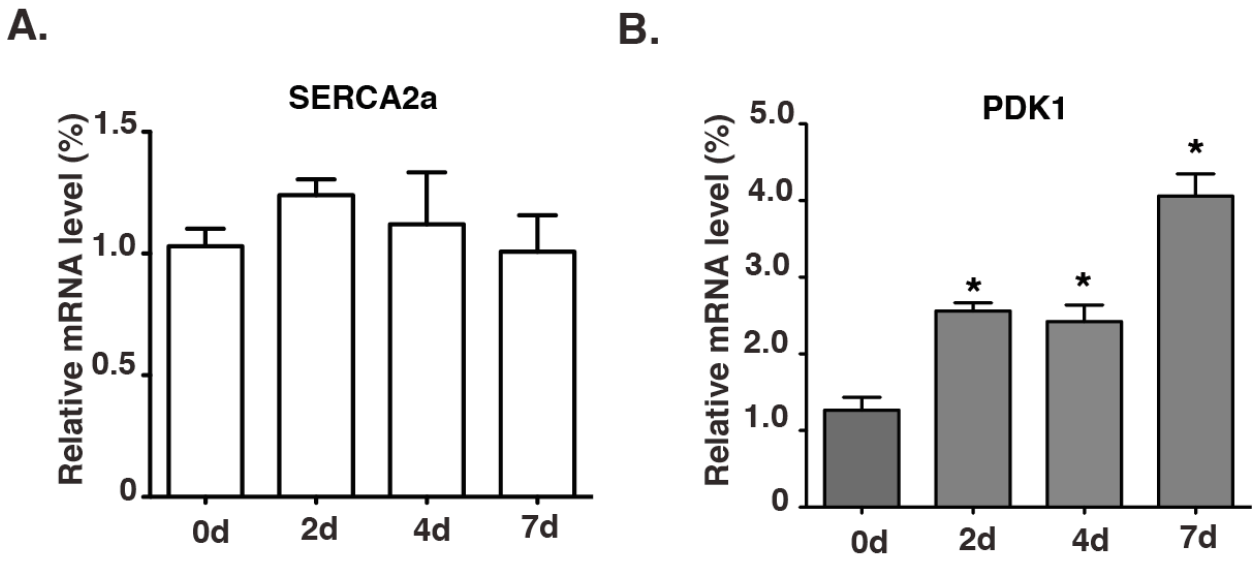

Figure S5. Depletion of PHD2/3 has no effect on SERCA2a expression and increases PDK1 expression. PHD2/3$^{f/f}$; Cre$^{+/-}$ mice were IP infused with tamoxifen for 5 consecutive days. At day 0, 2, 4 or 7 after the first infusion, mouse hearts were harvested and RNA were extracted. Real-time PCR were performed to determine the mRNA level of SERCA2a **(A)** or PDK1 **(B)** in the hearts. n = 4/time point, $^{*}p < 0.05$, compared to day 0, one way ANOVA.

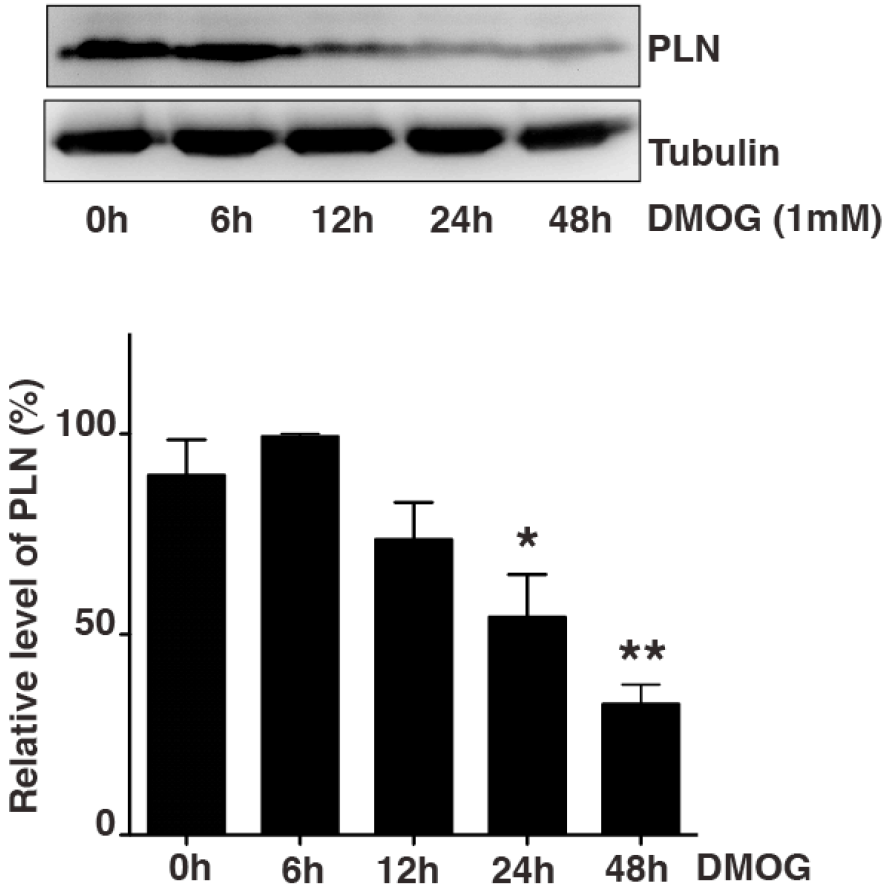

Figure S6. DMOG decreases the protein level of PLN in primary ventricular myocytes. Neonatal rat ventricular myocytes were treated with DMOG (1mM) as indicated. Cells were then harvested for western blots**.** Densitometry analysis from three experiments was shown**.** $^{*}p < 0.05$, $^{**}p < 0.01$, compared to 0h, one way ANOVA.

Ion Table & Error Map

#	b	b-H2O	b-NH3	b(2+)	Seq	y	y-H2O	y-NH3	y(2+)	#
1	88.04	70.03	71.01	44.52	S					24
2	201.12	183.11	184.1	101.06	L	2798.39	2780.38	2781.36	1399.69	23
3	329.18	311.17	312.16	165.09	Q	2685.30	2667.29	2668.27	1343.15	22
4	457.05	439.23	440.21	229.12	Q	2557.24	2539.23	2540.22	1279.12	21
5	613.3	595.33	596.32	307.17	R	2429.18	2411.17	2412.16	1215.09	20
6	710.39	692.38	693.37	355.7	P	2273.08	2255.07	2256.06	1137.06	19
7	839.43	821.43	822.39	420.22	E	2176.03	2158.02	2159	1088.52	18
8	952.66	934.49	935.49	476.74	P(+15.99)	2046.99	2028.98	2029.96	1024.01	17
9	1053.53	1035.52	1036.51	527.27	T	1933.94	1915.93	1916.91	967.47	16
10	1166.58	1148.57	1149.55	583.79	P(+15.99)	1832.89	1814.88	1815.87	916.95	15
11	1295.62	1277.61	1278.6	648.31	E	1719.84	1701.83	1702.82	860.42	14
12	1424.67	1406.66	1407.64	712.83	E	1590.8	1572.79	1573.78	795.9	13
13	1610.74	1592.73	1593.72	805.87	W	1461.76	1443.75	1444.73	731.38	12
14	1725.77	1707.76	1708.74	863.39	D	1275.66	1257.67	1258.65	638.34	11
15	1838.86	1820.85	1821.83	919.93	L	1160.66	1142.64	1143.63	580.83	10
16	1951.94	1933.93	1934.91	976.47	I	1047.57	1029.56	1030.54	524.28	9
17	2089	2070.99	2071.97	1045.01	H	934.49	916.49	917.46	467.75	8
18	2202.08	2184.07	2185.06	1101.55	I	797.43	779.42	780.4	399.21	7
19	2273.12	2255.11	2256.09	1137.06	A	684.34	666.33	667.32	342.67	6
20	2374.17	2356.16	2357.14	1187.58	T	613.3	595.29	596.28	307.15	5
21	2503.21	2485.2	2486.18	1252.11	E	512.26	494.25	495.23	256.63	4
22	2574.25	2556.24	2557.22	1287.61	A	383.22	365.2	366.19	192.11	3
23	2711.31	2693.3	2694.28	1356.14	H	312.18	294.17	295.15	156.59	2
24					R	175.12	157.11	158.09	88.06	1

Figure S7. TR-α is hydroxylated at proline residues P160 and P162. In vitro hydroxylation assay was performed with Flag-TR-α and recombinant PHD2 and 3. The protein band corresponding to TR-α was cut out for trypsin digestion. LC-MS/MS analysis was then performed to confirm the prolyl hydroxylation. The table lists the theoretical masses of all product ions from precursor peptides with matched masses indicated by the color code. N terminus–containing ions (b ions) are in blue and C terminus–containing ions (y ions) are in red.

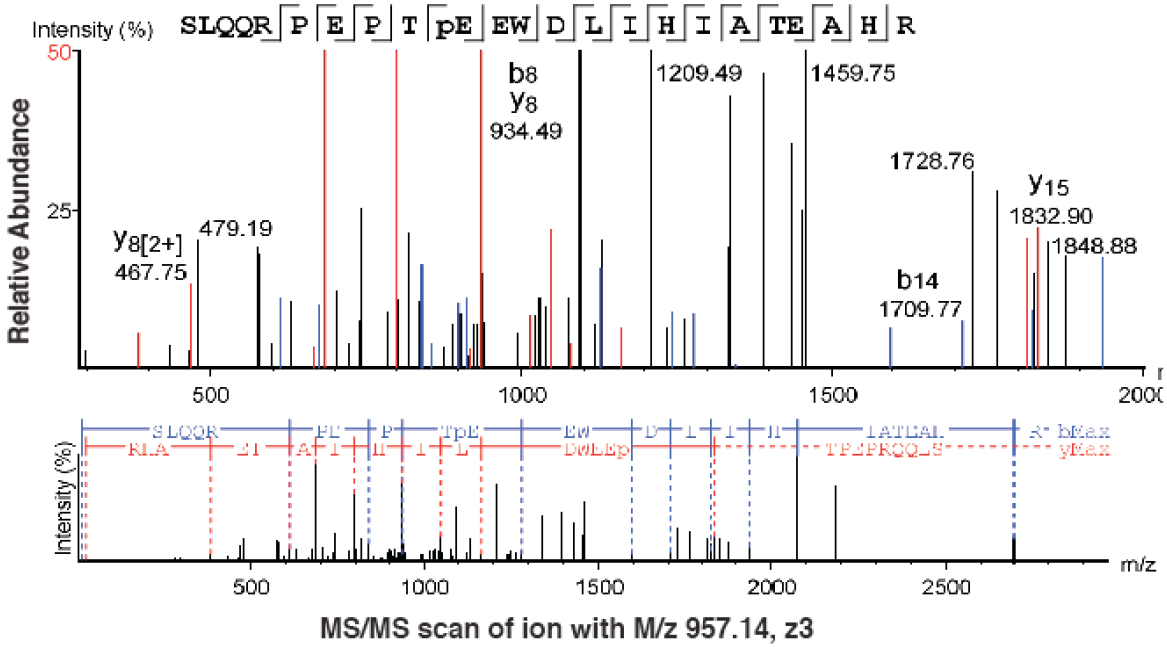

Ion Table & Error Map

#	b	b-H2O	b-NH3	b(2+)	Seq	y	y-H2O	y-NH3	y(2+)	#
1	88.04	70.03	71.01	44.52	S					24
2	201.12	183.11	184.1	101.06	L	2782.39	2764.38	2765.36	1391.7	23
3	329.18	311.17	312.16	165.09	Q	2669.31	2651.3	2652.28	1335.15	22
4	457.05	439.23	440.21	229.12	Q	2541.25	2523.24	2524.22	1271.12	21
5	613.32	595.33	596.32	307.17	R	2413.19	2395.18	2396.16	1207.09	20
6	710.39	692.38	693.37	355.7	P	2257.09	2239.08	2240.06	1229.07	19
7	839.44	821.43	822.39	420.22	E	2160.04	2142.03	2143.01	1080.54	18
8	936.47	918.48	919.46	468.75	P	2030.99	2012.98	2013.97	1016	17
9	1037.54	1019.53	1020.51	519.27	T	1933.94	1915.93	1916.91	967.47	16
10	1150.59	1132.58	1133.56	575.79	P(+15.99)	1832.9	1814.88	1815.79	916.95	15
11	1279.64	1261.62	1262.6	640.31	E	1719.84	1701.83	1702.82	860.42	14
12	1408.67	1390.66	1391.64	704.84	E	1590.8	1572.79	1573.78	795.9	13
13	1594.71	1576.74	1577.72	797.88	W	1461.76	1443.75	1444.73	731.38	12
14	1709.77	1691.77	1692.75	855.4	D	1275.66	1257.67	1258.65	638.34	11
15	1822.86	1804.85	1805.83	911.93	L	1160.66	1142.64	1143.63	580.83	10
16	1935.93	1917.93	1918.92	968.47	I	1047.57	1029.56	1030.54	524.28	9
17	2073.02	2054.99	2955.98	1037	H	934.49	916.49	917.46	467.75	8
18	2186.09	2168.08	2169.06	1093.54	I	797.43	779.42	780.4	399.21	7
19	2257.03	2239.11	2240.1	1129.07	A	684.34	666.33	667.32	342.67	6
20	2358.17	2340.16	2341.15	1179.59	T	613.3	595.29	596.28	307.15	5
21	2487.22	2469.21	2470.19	1244.12	E	512.26	494.25	495.23	256.63	4
22	2558.25	2540.24	2541.23	1279.64	A	383.22	365.2	366.19	192.11	3
23	2695.31	2677.3	2678.28	1348.16	H	312.18	294.17	295.15	156.59	2
24					R	175.12	157.11	158.09	88.06	1

Figure S8. TR-α is hydroxylated at proline residues P162. In vitro hydroxylation assay was performed with Flag-TR-α and recombinant PHD2 and 3. The protein band corresponding to TR-α was cut out for trypsin digestion. LC-MS/MS analysis was then performed to confirm the prolyl hydroxylation. Tandem mass spectrum of the precursor ion at m/z = 957.14 (z=3) for human TR-α 153-176 sequence SLQQRPEPTP (+15.99) EEWDLIHIATEAHR were shown. The peak heights are the relative abundances of the corresponding fragment ions, with the annotation of the identified

matched N terminus–containing ions (b ions) in blue and C terminus–containing ions (y ions) in red. Fragment ions at M/z=1279.64 (b11), M/z=1832.90 (y15) & M/z=916.95 $(b15)^{2+}$ represent characteristic ions that unambiguously identify P162 hydroxylation. The table lists the theoretical masses of all product ions from precursor peptides with matched masses indicated by the color code. N terminus–containing ions (b ions) are in blue and C terminus–containing ions (y ions) are in red.

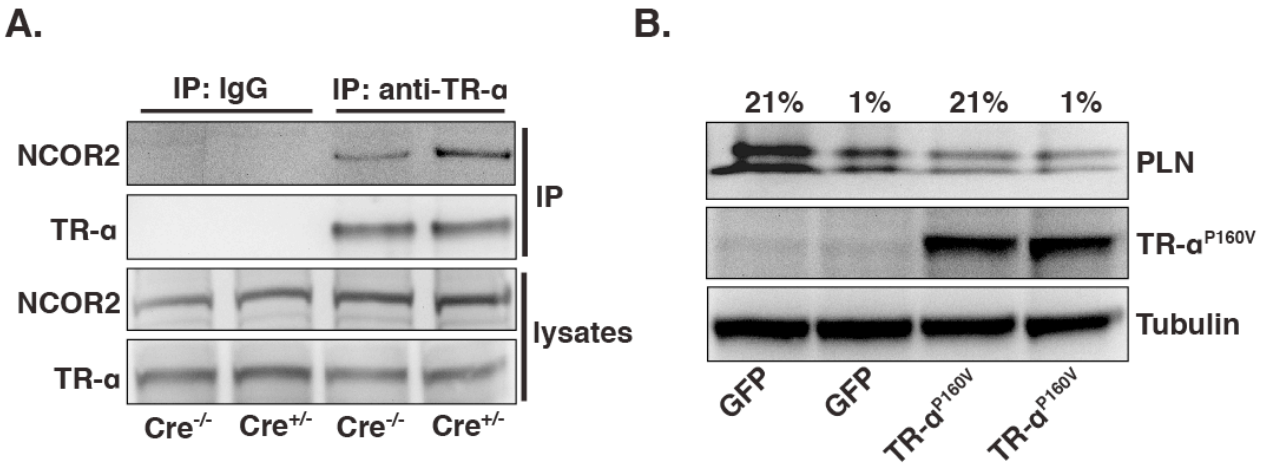

Figure S9. Depletion of PHD2/3 promotes the interaction between TR-α and NCOR2 and TR-α^{P160V} decreases the protein level of PLN. (A) PHD2/3$^{f/f}$; Cre$^{-/-}$ or PHD2/3$^{f/f}$; Cre$^{+/-}$ mice were IP injected with tamoxifen for 5 days. At day 7, mouse hearts were harvested and Co-IP were performed with anti-TR-α antibody. Western blots were then performed as indicated. **(B)** Neonatal rat ventricular myocytes were infected with lentivirus expressing Flag-TR-α^{P160V} for 2 days and then treated with hypoxia (1% O_2) as indicated for 24 hours. Cells were harvested and western blots were performed.

Figure S10. Protein sequence alignment of human TR-α and TR-β. PEP motif (in Green) is conserved between TR-α and TR-β, however, the N-terminal sequences of this motif are completely different except one serine.

GeneSymbol	Description	FC	FDR
Sprr1a	small proline-rich protein 1A	5.5	0.0%
Tnnt3	troponin T3, skeletal, fast	5.2	0.0%
Ltbp2	latent transforming growth factor beta binding protein 2	5.1	0.0%
Crlf1	cytokine receptor-like factor 1	4.8	3.5%
Col9a2	collagen, type IX, alpha 2	4.6	0.0%
Postn	periostin, osteoblast specific factor	4.6	0.0%
Nmrk2	nicotinamide riboside kinase 2	4.6	0.0%
Col8a2	collagen, type VIII, alpha 2	4.6	0.0%
Ddah1	dimethylarginine dimethylaminohydrolase 1	4.5	0.0%
Myh7	myosin, heavy polypeptide 7, cardiac muscle, beta	4.4	0.0%
Thbs4	thrombospondin 4	4.3	0.0%
Slc16a3	solute carrier family 16	4.2	0.0%
Kcnv2	potassium channel, subfamily V, member 2	-3.5	0.0%
Efnb3	ephrin B3	-3.5	3.5%
Cngb3	cyclic nucleotide gated channel beta 3	-3.4	0.0%
Cyp26b1	cytochrome P450, family 26, subfamily b, polypeptide 1	-3.4	1.5%
2310007J06Rik	adult male tongue cDNA AK009210	-3.4	3.5%
Kcnip2	Kv channel-interacting protein 2	-3.4	3.5%
Ogdhl	oxoglutarate dehydrogenase-like	-3.3	0.0%
Fbp2	fructose bisphosphatase 2	-3.2	0.0%
Lgals4	lectin, galactose binding, soluble 4	-3.1	3.5%
Adhfe1	alcohol dehydrogenase, iron containing, 1	-3.1	0.0%
Rpl3l	ribosomal protein L3-like	-3.0	0.0%
Slc26a10	solute carrier family 26	-3.0	0.0%

Table S1: The top 12 genes that increase (red, top) or decrease (blue, bottom) in hearts from PHD2/3$^{f/f}$; Cre$^{+/-}$ relative to PHD2/3$^{f/f}$; Cre$^{-/-}$ mice. The official gene symbol and brief description for each gene are provided. The fold change (FC) is the difference (log base 2) comparing PHD2/3$^{f/f}$; Cre$^{+/-}$ to PHD2/3$^{f/f}$; Cre$^{-/-}$ samples. The false discovery rate (FDR, q-value) is also provided for each gene. For a full list of the 2500 differentially expressed genes with a relative fold change > 2 comparing PHD2/3$^{f/f}$; Cre$^{+/-}$ to PHD2/3$^{f/f}$; Cre$^{-/-}$samples is accessible through the National Center for Biotechnology Information (NCBI) Gene Expression Omnibus (GEO), accession number GSE67726.

Pathway	p-value	Matched Entities	Total Entities
Glycolysis and Gluconeogenesis (WP157 r78433)	7.10E-31	19	50
TCA Cycle (WP434 r70013)	4.54E-24	24	31
Fatty Acid Beta Oxidation (WP1269 r72137)	3.04E-15	19	34
Oxidative phosphorylation (WP1248 r69092)	7.12E-12	22	59
XPodNet - protein-protein interactions in the podocyte (WP2309 r72004)	3.21E-11	103	836
Electron Transport Chain (WP295 r79459)	5.11E-11	37	102
Cell cycle (WP190 r71755)	7.08E-11	25	88
G1 to S cell cycle control (WP413 r78432)	1.39E-10	20	62
Mitochondrial LC-Fatty Acid Beta-Oxidation (WP401 r71751)	2.80E-09	10	16
Fatty acid oxidation (WP2318 r73549)	1.98E-08	8	11
Fatty Acid Biosynthesis (WP336 r71737)	1.63E-07	10	22
PodNet- protein-protein interactions in the podocyte (WP2310 r72005)	2.35E-07	43	315
p53 signaling (WP2902 r79094)	2.86E-07	17	109
DNA Replication (WP150 r69148)	3.61E-07	13	41
B Cell Receptor Signaling Pathway (WP274 r67072)	1.45E-06	26	156
Focal Adhesion (WP85 r78289)	8.90E-06	27	185
miRNA regulation of DNA Damage Response (WP2087 r78434)	2.02E-05	14	91
Kit Receptor Signaling Pathway (WP407 r69079)	1.24E-04	13	67
Focal Adhesion-PI3K-Akt-mTOR-signaling pathway (WP2841 r79327)	2.89E-04	35	327
Apoptosis (WP1254 r69153)	3.25E-04	14	83
Nucleotide Metabolism (WP87 r71749)	5.73E-04	6	19
Polyol pathway (WP1265 r69077)	7.76E-04	3	4
Myometrial Relaxation and Contraction Pathways (WP385 r72108)	8.63E-04	20	157
Chemokine signaling pathway (WP2292 r72463)	1.09E-03	22	193

Table S2: The top 24 pathways enriched in PHD2/3$^{f/f}$; Cre$^{+/-}$ relative to PHD2/3$^{f/f}$; Cre$^{-/-}$ mouse hearts. The wikipathway (WP) identifier and revision number (r) is provided. The results of Single Experiment Analysis (SEA) pathway enrichment analysis (Genespring v13.0, Agilent) calculated by comparing the number of expected pathway genes as distributed in the mouse genome to the genes identified as differentially expressed in our analysis is provided. Additionally, the number of matched differentially expressed entities (Matched Entities) and the total number entities in the curated pathway (Total Entities) are included.